

DTIC FILE COPY

(2)

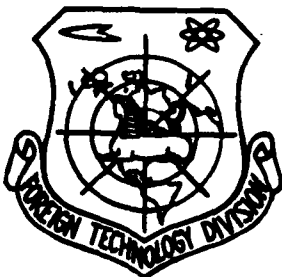
FTD-ID(RS)T-0977-88

FOREIGN TECHNOLOGY DIVISION



CHINESE JOURNAL OF SPACE SCIENCE  
(Selected Articles)

AD-A203 978



DTIC  
SELECTED  
3 FEB 1989  
S E D

Approved for public release;  
Distribution unlimited.



89 2 3 021

## **HUMAN TRANSLATION**

**FTD-ID(RS)T-0977-88**

**5 January 1989**

**MICROFICHE NR: FTD-89-C-000010**

**CHINESE JOURNAL OF SPACE SCIENCE (Selected  
Articles)**

**English pages: 14**

**Source: Kongjian Kexue Xuebao, Vol. 8, Nr. 2,  
April 1988, pp. 133-137; 145-149**

**Country of origin: China**

**Translated by: Leo Kanner Associates  
F33657-88-D-2188**

**Requester: FTD/WE**

**Approved for public release; Distribution unlimited.**

THIS TRANSLATION IS A RENDITION OF THE ORIGINAL FOREIGN TEXT WITHOUT ANY ANALYTICAL OR EDITORIAL COMMENT. STATEMENTS OR THEORIES ADVOCATED OR IMPLIED ARE THOSE OF THE SOURCE AND DO NOT NECESSARILY REFLECT THE POSITION OR OPINION OF THE FOREIGN TECHNOLOGY DIVISION.

PREPARED BY:

TRANSLATION DIVISION  
FOREIGN TECHNOLOGY DIVISION  
WPAFB, OHIO.

*Partial contents:*

TABLE OF CONTENTS

|  |    |
|--|----|
| Graphics Disclaimer .....  | ii |
| Difference in Spread-F at Haikou and Huancayo Stations; by Han Fufen,<br>Huang Changli ..... | 1  |
| Frequency Prediction by Oblique Ionogram, by Zhao Delin .....                                | 8  |

|                    |                                     |
|--------------------|-------------------------------------|
| Accession For      |                                     |
| NTIS GRA&I         | <input checked="" type="checkbox"/> |
| DTIC TAB           | <input type="checkbox"/>            |
| Unannounced        | <input type="checkbox"/>            |
| Justification      |                                     |
| By _____           |                                     |
| Distribution/      |                                     |
| Availability Codes |                                     |
| Avail and/or       |                                     |
| Dist               | Special                             |

A-1



→ Kipunzi, Soni, Taita, Maa, etc;  
Suriats, Sengwer, Suriat, etc.  
Diorne, Yala, etc., Chinese transcribers,  
(ed.)

**GRAPHICS DISCLAIMER**

All figures, graphics, tables, equations, etc. merged into this translation were extracted from the best quality copy available.

## DIFFERENCE IN SPREAD-F AT HAIKOU AND HUANCAYO STATIONS

Han Fufen and Huang Changli  
China Research Institute of Radiowave Propagation

### Abstract

The paper statistically analyzes the local time, seasonal and solar cycle variations of frequency spread-F at Haikou Station during years of maximum and minimum sunspots. It was found that the occurrence rate of frequency spread-F at Haikou has some variation rule with the local time, seasonal and solar cycle variations. Comparisons were made between the Haikou and the Huancayo stations; differences are pointed out in frequency spread-F at these two stations.

### I. FOREWORD

Many authors have reported the status [1-3] of frequency spread-F in the equator zone. Generally speaking, months of the most frequently occurrence of frequency spread-F are November and December in the equator zone in South America, and June and July in the equator zone in Asia. However, there are exceptions. For example, the least frequent occurrences of frequency spread-F are June and July at the Legon Station [5 degrees N]; however, there is no apparent seasonal variation of frequency spread-F at Kodaikanal Station [6 degrees N] [5].

The paper statistically analyzes the frequency spread-F data of maximum (1981, 1980, 1969 and 1959) and minimum sunspot years (1976, 1975, 1974, 1965 and 1964) at Haikou Station (110.3

degrees E, 20.0 degrees N, and 8.5 degrees N in magnetic latitude). Moreover, the frequency spread-F data of maximum (1967, 1968, 1969, 1970 and 1971) and minimum sunspot years (1962, 1963, 1964, 1973 and 1974) at Huancayo Station (75.3 degrees W, 12 degrees S, and 2 degrees N in magnetic latitude) were obtained from reference [3]. The authors compared the states of frequency spread-F of these two stations; there are many differences. In the following, differences in frequency spread-F states of these two stations are described one by one.

## II. Difference in Nocturnal Variation of Frequency Spread-F

Figure 1 shows that there are differences in nocturnal variation of spread-F at these two stations with local time.

During maximum sunspot years, the occurrence of frequency spread-F is maximum between 2000 and 2100 h LT (local time) at Haikou Station; later, the occurrence rate gradually decreases, with an average occurrence rate of 17 percent. The nocturnal variation of frequency spread-F in 1969 also follows this rule basically. In minimum sunspot years, the highest value of frequency spread-F occurrence is 2300 to 0400 h LT with an average occurrence rate at 21 percent.

At the Huancayo Station, in both the maximum and minimum sunspot years, the frequency spread-F gradually increases from 1845 h LT to its maximum value near midnight between 2300 and 0100 h LT. Thereafter, the frequency spread-F gradually decreases. In the maximum sunspot years, the average occurrence rate is 20 percent; the average occurrence rate is 19 percent in the minimum sunspot years. As mentioned above, there are differences in occurrence probability of frequency spread-F at these two stations in different solar activation periods. There are different local times of occurrence of the highest value of frequency spread-F.

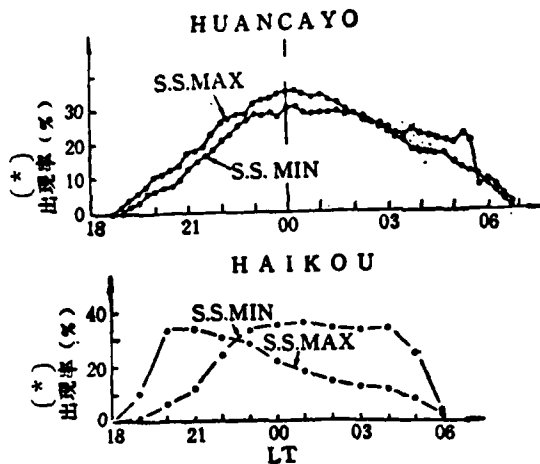


Fig. 1. The Average Nocturnal Variations of Frequency Spread-F at Haikou and Huancayo Stations During Years of Maximum and Minimum Sunspots.

Key: \*Occurrence rate (%).

The following can be seen from Fig. 2: (1) In periods of equinoxes (March, April, September and October), there are more occurrences of frequency spread-F at Haikou Station during the maximum sunspot years; the highest value of the occurrence rate is 75 percent. The occurrence rate is less frequent in minimum sunspot years; the highest value of occurrence rate is only 26 percent. At Huancayo Station, whatever the maximum or the minimum sunspot years, basically the occurrence rate is the same; the maximum value is approximately 30 percent. It can be seen from the figure (Fig. 2) that the highest occurrence probability of frequency spread-F at Haikou Station is 50 percent higher in the maximum sunspot years over the minimum sunspot years; at Huancayo Station, the value is 40 percent higher. There are different occurrence times of frequency spread-F at these two stations. (2) In the local summer periods, since there are different positions for these two stations (summer at Haikou

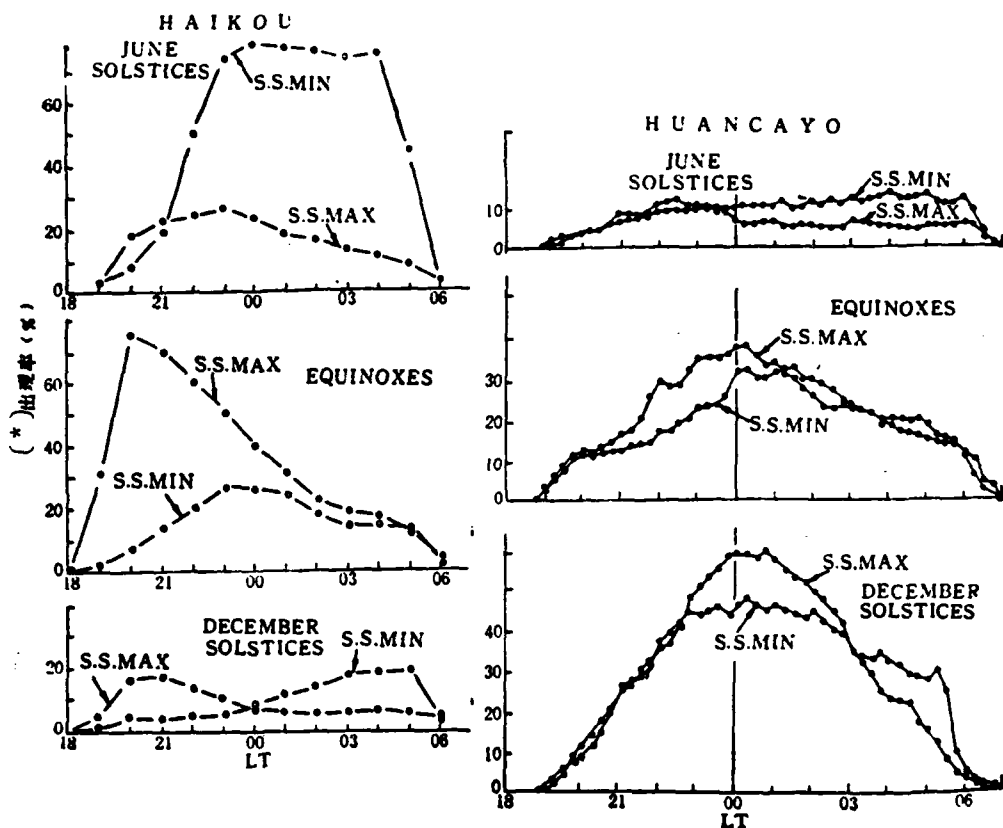


Fig. 2. The Average Nocturnal Variations of the Occurrence of Frequent Spread-F at Haikou and Huancayo During Different Seasons of Maximum and Minimum Sunspot Years.

Key: \* Occurrence rate (%).

is between May and August while summer at Huancayo is the period of November, December, January and February), at Haikou Station there is more occurrence of spread-F in the minimum sunspot years; the highest value of the occurrence rate is 70 percent. In the maximum sunspot years, there is relatively less occurrence of spread-F; the highest value of the occurrence rate is only 20 percent. At Huancayo Station, the occurrence of frequency spread-F is relatively more often in both the maximum and minimum sunspot years. (3) In the local winter period (winter months at Haikou are November, December, January and February while winter months at Huancayo are May through August), there is very

infrequent occurrence of frequency spread-F in both the maximum and minimum sunspot years; however, there are different nocturnal variations.

The authors detected two significant features for spread-F at Haikou Station. One feature is a very high occurrence rate of spread-F at 2300 to 0400 h LT in summer in the minimum sunspot years. The second feature is a very high occurrence rate of spread-F at 2000 to 2100 h LT in months of equinoxes in the maximum sunspot years.

### III. Differences of Seasonal Variation of Frequency Spread-F

It is apparent from Fig. 3 that at Haikou Station there is relatively greater occurrence of frequency spread-F in the season of equinoxes; the highest value of the occurrence rate is between 70 and 80 percent. At Huancayo Station, relatively greater occurrence of spread-F is during the local summer season; the highest value of the occurrence rate is between 60 and 70 percent. In the minimum sunspot years, greater occurrence of spread-F at Haikou and Huancayo stations is during the local summer season; the highest value of the occurrence rate is 70 to 80 percent at Haikou Station, and 50 to 60 percent at Huancayo Station. At these two stations, the occurrence rate of frequency spread-F is slightly higher at Haikou than at Huancayo station in both the maximum and minimum sunspot years.

### IV. Conclusions

With comparative analysis on data at Haikou and Huancayo stations, it can be seen that there is a significant difference for the frequency spread-F feature at Haikou and Huancayo stations. From the nocturnal variation of spread-F, in the maximum sunspot years, the occurrence of the highest value of frequency spread-F at Haikou Station is at 2000 h LT while the

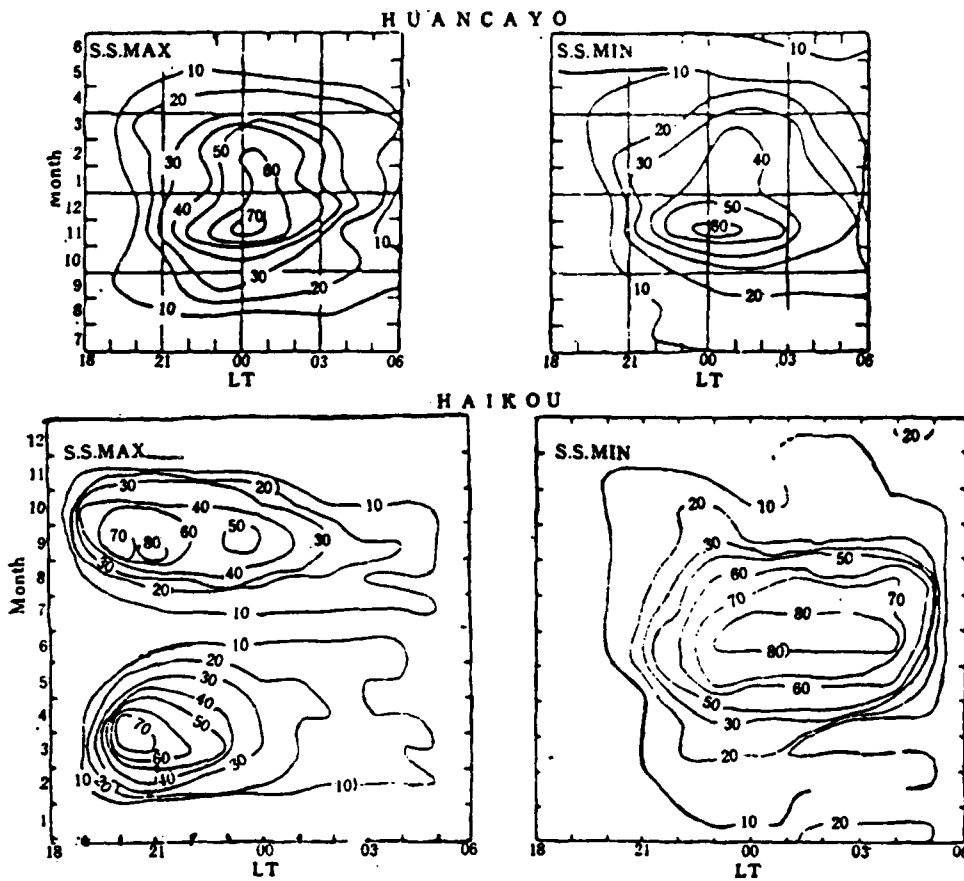


**Figure 3.** Contours of Constant Occurrence Probability of Frequency Spread-F at Haikou and Huancayo During Years of Maximum and Minimum Sunspots Plotted on a Grid of Local Time and Months of the Year.

highest value at Huancayo Station occurs at 0000 h LT. In the minimum sunspot years, the highest occurrence value of frequency spread-F at Haikou Station is from 2300 to 0400 LT; at Huancayo Station, the highest value occurs at 0000 LT, and then the value gradually declines. In seasonal variation, occurrence of spread-F at Haikou Station is higher during equinoxes in the maximum sunspot years; in the local summer season in the minimum sunspot years, the occurrence is higher. At Huancayo Station, the highest occurrence months of spread-F are in the local summer season in both the maximum and minimum sunspot years.

The paper was received for publication on 5 August 1987.

## BIBLIOGRAPHY

- [ 1 ] Lyon, A. J., N. J. Skinner and W. J. Wright, *J. Atmos. Terr. Phys.*, Vol. 21, p. 100, 1961.
- [ 2 ] Chandra, H. and R. G. Rastogi, *Ann. Geophys.*, Vol. 28, p. 37, 1972.
- [ 3 ] Rastogi, R. G. *J. Atmos. Terr. Phys.*, Vol. 42, p. 593, 1980.
- [ 4 ] Basu, S. and M. C. Kelley, *Radio Sci.*, Vol. 14, p. 471, 1979.
- [ 5 ] Rastogi, R. G., *J. Geophys. Res.*, Vol. 85, p. 722, 1980A.

## FREQUENCY PREDICTION BY OBLIQUE IONOGRAM

Zhao Delin  
China Research Institute of Radiowave Propagation

### Abstract

The paper analyzes an oblique (P-f) ionogram. Based on an interpretative reading of the obtained ionogram, the day to day variation curve of the highest observed frequency is plotted; the curve can be considered as quasireal time frequency prediction curve of the ionosphere. The ionosphere simultaneously provides several important ionosphere prediction parameters, such as MOF, LOF, MUF and effects of Es. In the later sections of the paper, backscattering and oblique ionograms (measured simultaneously on a single ionogram) are combined to give the window of optimal operating frequency. The result can be used as the basis of revised long range forecasting on a fixed communication line because the long range forecasting is converted from vertical sounding data.

### I. FOREWORD

From April to May 1985, a joint observation experiment of ionosphere oblique detection and backscattering was conducted along China's northwest communication line (Xinxiang to Jiuquan); a backscattering instrument was installed at Xinxiang, and a synchronous sweep frequency responder was installed at Jiuquan. The large circle distance of the communication line is 1,435 kilometers.

This is a pulse system in the following operating mode: A sweeping transmission is made once every 15 minutes by the sweep frequency backscattering instrument, which was installed at Xinxiang; the range of the sweeping frequency is between 3 and 30 MHz with sweeping frequency time at 4 minutes and 30 seconds, sweeping mode at step type, sweeping rate at 100 kHz/s for each step, repetition frequency at 15 Hz/s and pulse width at 100 microseconds. After the Jiuquan sweep frequency responder receives pulse signals transmitted from Xinxiang with a time delay of 1 millisecond, a pulse signal (actually an oblique detection signal) of the same frequency is transmitted. After the Xinxiang backscattering instrument receives these signals, a frame of an oblique ionogram is shown on a display. The oblique ionogram and the trace (the backscattering ionogram) through backscattering from the ground surface appear simultaneously on an ionogram [1], as shown in Fig. 1.

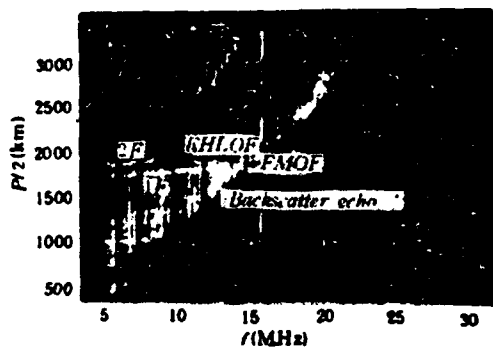


Fig. 1. Trace of Backscattering and Oblique Ionogram

An oblique trace and a backscatter minimum time delay trace are visible clearly from the photographic film. It should be pointed out that the oblique trace actually should be at 150 kilometers beneath the trace displayed from the ionogram, because the pulse of the same frequency is retransmitted by the responder after a time delay of 1 millisecond.

After a time check with a shortwave time reporting station, the system time synchronization is established through a backscattering instrument signal captured by the sweep frequency responder. The transmission power of the backscattering instrument is 15 kilowatts, using a log-periodic antenna array. The transmission power of the responder is 1 kilowatt, using an inverted V type antenna.

## II. Frequency Forecasting

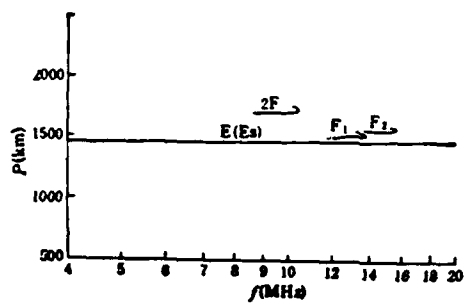
The frequency prediction curve is given by the experimentally obtained oblique ionogram. Used as a reference for interpretative reading of an oblique ionogram, a vertical sounding ionogram at 11.15 hours on 14 April 1985 at the midpoint (Lanzhou) of ionosphere and a family of transmission curves [2] corresponding to 1,435 kilometers were used. In addition, equivalent equations of the plane ionosphere are applied:

$$f_{ob} = f_V \sec \phi_0, \quad (1)$$

$$P(f_{ob}) = 2h'(f_V) \sec \phi_0, \quad (2)$$

to calculate an oblique ionogram;  $f_{ob}$  is the oblique projection frequency (corresponding to the observed frequency in the experiment);  $f_V$  is the equivalent vertical sounding frequency;  $\phi_c$  is the incident angle of oblique projection;  $P(f_{ob})$  is the signal group path of oblique detection; and  $h'$  is the pseudoheight. P-f curves of various modes thus estimated are shown in Fig. 2. The result is similar to a real oblique ionogram obtained experimentally [3].

In experiments, four ionograms are obtained each hour, and 96 ionograms each day. By interpretative readings on these ionograms,  $f_{ob}$  day to day variation curves of various transmission modes can be obtained. Fig. 3 shows one of these



$D = 1435 \text{ km}$ ,  $f_0E = 3.2 \text{ MHz}$ ,  $A'E = 110 \text{ km}$ ,  $f_0F_1 = 4.5 \text{ MHz}$ ,  
 $A'F_1 = 200 \text{ km}$        $f_0F_2 = 6.8 \text{ MHz}$ ,  $A'F_2 = 300 \text{ km}$

Figure 2. Oblique Ionogram  
Calculated Transmission  
Curve for a Fixed Distance  
1,435 km

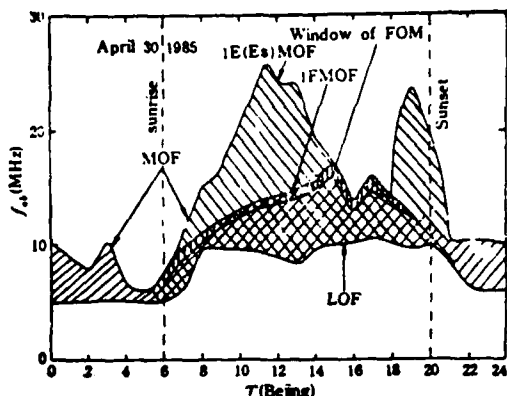


Figure 3. Day to Day Variation  
of Observed Frequency

day to day variation curves; the curve is obtained through interpretative reading on these 96 ionograms obtained on 30 April 1985. Figure 3 presents many important transmission parameters (MOF, LOG and EsMOF) of the ionosphere, including displaying the window of optimal operating frequency. Also from Fig. 3, transmission modes (such as E, Es, E(Es) and F mixed mode [4]) can be seen as they appeared at different time periods. Based on prediction requirements, in the figure the transmission mode of the lower frequency terminal is eliminated. In the lower end of the frequency, actually there are more complex modes which are more difficult to read interpretatively. However, there is little affecting the frequency prediction. Thus, only doing interpretative reading on ionograms obtained every day, the real time frequency prediction result can be obtained everyday.

### III. Analysis of Results

As seen from day to day variation curves of the observed frequency, communication is difficult and more intensive interference may occur from 21.00 hours at night to 0600 hours the next morning. The frequency range for selection is relatively narrow for communication, generally only about 4 MHz.

✓ 11

Communication is even more difficult around 0500 hours; communication can be maintained only with relatively low frequency, with about 1 MHz of frequency range available for selection. Communication improves rapidly after 0600 hours after sunrise with transmission of the E(Es) mode. Thereafter, transmission modes become more complex. Before and after midday, communication is more adaptable to using the E(Es) layer. Since the experiments were conducted in April and May, the probability of Es occurrence is greater and more intensive. Therefore the highest observed Es MOF frequency of the Es layer is usually higher than the highest observed F2 MOF frequency of the F2 layer. Near midday, sometimes Es MOF can be 10 MHz higher than F2 MOF. When Es is more intensive, the Es mode can be used for fast information transmission at higher frequencies because at that time the time difference  $\Delta T$  of the transmission signal is considerably decreased, approaching zero for multipath scattering. If the operating frequency is appropriately selected, the transmission rate can be considerably increased, by 100-fold higher than for the general situation in the opinion of some researchers. As revealed in observations, the time percentage of communication is between 30 and 40% when using Es at daytime in April and May. Of course, in the daytime the highest observation frequency of the F2 layer is high. When Es is relatively weak, it is also relatively ideal to use the F2 mode for data transmission because the signal time difference  $\Delta T$  is also very small in the vicinity of F2 MOF, since the maximum transmission rate is roughly equal to the reciprocal of the multipath transmission time difference  $\Delta T$ . Hence, it is very important for real time data communication to select the highest observation frequency. This is the excellence of the oblique detection system because frequency prediction can be timely given on a fixed communication line. The Es layer also appears before and after sunset; Es MOF is also considerably higher than F2 MOF. Hence it is relatively satisfactory to use the Es layer for transmission at that time.

In the following, a further analysis is made of selecting the window of the optimal operating frequency. As described above, the backscattering ionogram is simultaneously displayed on the obtained oblique ionogram. In the vicinity of the minimum time delay curve on the backscattering ionogram, there are more intensive traces of scattering echo traces. This type of echo enhancement is, on the one hand, caused by jump distance focusing of high and low radiowave rays (transmitted through the ionosphere) in the vicinity of the minimum time delay curve. On the other hand, it is caused by time focusing of the ground object echo in the vicinity of the minimum time delay curve. Hence, echo enhancement also reveals the range of the more intensive focusing zone in addition to revealing the transmission jump distance. It can be seen that the transmission mode gradually transfers from multimode to monomode with increasing detection frequency; at the same time, the range of the focusing zone is decreased (Fig. 1). As indicated by an interpretative reading of a large number of ionograms, traces at the connecting place of oblique detection high and low radiowave rays fall in the vicinity of the minimum time delay curves of backscattering. This matches well with the prediction result. Generally, the connection frequency is termed the classic MUF. Thus, the highest usable MUF frequency can be conveniently determined, relying on oblique detection and backscattering traces. At the same time, the corresponding frequency range of the more intensive echo traces of an oblique path can be determined. Corresponding to the black band width in Fig. 3, this frequency range can approximately reveal the range of optimal operating frequency; this is called the window of the optimal operating frequency in the paper. As in higher frequencies, only the F2 layer can generate focusing; Es is a thin layer and generally does not produce focusing. Therefore the minimum time delay curve is the focusing trace of the Fe layer. It should be pointed out that sometimes in observation the oblique detection trace exceeds the minimum time delay trace (on the frequency

axis). These oblique detection traces are produced through Es layer transmission. Based on the above mentioned analyses, Es MOF in Fig. 3 is obtained. Of course, the scattering transmission of the ionosphere may also produce peersen rays exceeding the connection frequency. No detailed analysis is made in the paper.

#### IV. Discussion of Results

The more intensive scattering echo wave in the vicinity of the minimum time delay curve is related to ground scattering characteristics beside focusing. When the ground scattering is more intensive, the backscattering trace may also be intensified. However, this enhancement cannot be distinguished from the echo enhancement zone caused by focusing. Therefore, there are difficulties in interpretative reading, thus leading to errors.

In addition, the delay time of the responder should be greater; thus, the oblique detection traces fall onto signals without backscattering to facilitate interpretative reading in order to reduce error.

The paper was received for publication on 3 November 1987.

#### BIBLIOGRAPHY

- [1] Wright, J. W., *Trans. IEEE*, AP-16, p. 217, 1968.
- [2] Davies, K., *Ionospheric Radio Propagation*, National Bureau of Standards Monograph 80, p. 165, 1965.
- [3] Wilkins, A. F. and E. D. R. Shearman, *J. Brit. IRE*, Vol. 17, p. 601, 1957.
- [4] N. Narayana Rao, *Radio Sci.*, Vol. 9, p. 845, 1974.

DISTRIBUTION LIST  
DISTRIBUTION DIRECT TO RECIPIENT

| <u>ORGANIZATION</u>    | <u>MICROFICHE</u> |
|------------------------|-------------------|
| A205 DMAHTC            | 1                 |
| A210 DMAAC             | 1                 |
| C509 BALLISTIC RES LAB | 1                 |
| C510 R&T LABS/AVEADCOM | 1                 |
| C513 ARRAADCOM         | 1                 |
| C535 AVRADCOM/TSARCOM  | 1                 |
| C539 TRASANA           | 1                 |
| C591 FSTC              | 4                 |
| C619 MIA REDSTONE      | 1                 |
| D008 MISC              | 1                 |
| E053 HQ USAF/INET      | 1                 |
| E404 AEDC/DCF          | 1                 |
| E408 AFWL              | 1                 |
| E410 AD/IND            | 1                 |
| E429 SD/IND            | 1                 |
| P005 DOE/ISA/DDI       | 1                 |
| P050 CIA/OCR/ADD/SD    | 2                 |
| AFIT/LDE               | 1                 |
| FTD                    | 1                 |
| CCV                    | 1                 |
| MIA/PHS                | 1                 |
| LLNL/CODE L-389        | 1                 |
| NASA/NST-44            | 1                 |
| NSA/T513/TDL           | 2                 |
| ASD/FTD/TQLA           | 1                 |
| FSL/NIX-3              | 1                 |